Proceedings of the Combustion Institute 34 (2013) 1939–1947
H. Nakayama, J. Kasahara, A. Matsuo, I. Funaki

Title: **Front shock behavior of stable curved detonation waves in rectangular-cross-section curved channels**

Authors: HISAHIRO NAKAYAMA[1], JIRO KASAHARA[1], AKIKO MATSUO[2], IKKOH FUNAKI[3]

Affiliation 1: Department of Engineering Mechanics and Energy, University of Tsukuba
1-1-1 Tennodai, Tsukuba, Ibraki 305-8573, Japan

Affiliation 2: Department of Mechanical Engineering, Keio University
3-14-1 Hiyoshi, Kouhoku-ku, Yokohama, Kanagawa 223-8522, Japan

Affiliation 3: Institute of Space and Astronautical Science, Japan Aerospace Exploration Agency
3-1-1 Yoshinodai, Chuo-ku, Sagamihara, Kanagawa 252-5210, Japan

Address: JIRO KASAHARA, Department of Engineering Mechanics and Energy, University of Tsukuba
1-1-1 Tennodai, Tsukuba, Ibaraki 305-8573, Japan
E-mail: kasahara@kz.tsukuba.ac.jp
Fax: 029-853-5267

Colloquium: DETONATIONS, EXPLOSIONS AND SUPERSONIC COMBUSTION including pulse-detonation and scramjet engines

Total Length: 6197 words
(Method: M1)

Main text:	2568 words
Nomenclature:	113 words
References:	340 words
Tables:	99 words
Figures:	3077 words

Abstract

The propagation of curved detonation waves of gaseous explosives stabilized in rectangular-cross-section curved channels is investigated. Three types of stoichiometric test gases, $C_2H_4+3O_2$, $2H_2+O_2$, and $2C_2H_2+5O_2+7Ar$, are evaluated. The ratio of the inner radius of the curved channel (r_i) to the normal detonation cell width (λ) is an important factor in stabilizing curved detonation waves. The lower boundary of stabilization is around r_i/λ=23, regardless of the test gas. The stabilized curved detonation waves eventually attain a specific curved shape as they propagate through the curved channels. The specific curved shapes of stabilized curved detonation waves are approximately formulated, and the normal detonation velocity (D_n) − curvature (κ) relations are evaluated. The D_n nondimensionalized by the Chapman-Jouguet (CJ) detonation velocity (D_{CJ}) is a function of the κ nondimensionalized by λ. The $D_n/D_{CJ}-\lambda\kappa$ relation does not depend on the type of test gas. The propagation behavior of the stabilized curved detonation waves is controlled by the $D_n/D_{CJ}-\lambda\kappa$ relation. Due to this propagation characteristic, the fully-developed, stabilized curved detonation waves propagate through the curved channels while maintaining a specific curved shape with a constant angular velocity. Self-similarity is seen in the front shock shapes of the stabilized curved detonation waves with the same r_i/λ, regardless of the curved channel and test gas.

Keywords

Curved detonation wave, Curvature, Normal detonation velocity, Cell width, Rotating detonation engine

Nomenclature

D: detonation velocity

m: exponent in Eq. (3)

p: pressure

r: distance from the polar coordinate origin to an arbitrary point on the detonation wave

t: time

Greek symbols

ϕ: angular difference between rotational and tangential directions at an arbitrary point on the detonation wave

κ: detonation wave curvature

λ: normal detonation cell width

θ: angle from the initial line to an arbitrary point on the detonation wave

τ: nondimensional time

ω: angular velocity of an arbitrary point on the detonation wave

Subscripts

0: initial condition

asy: asymptotic value at sufficiently large r

CJ: Chapman-Jouguet

i: inner wall of a curved channel

n: normal direction

o: outer wall of a curved channel

1. Introduction

Since a rotating detonation engine (RDE) [1−4] utilizes a combustible gas mixture as a propellant and its combustor is annular, a curved detonation wave propagating continuously is seen in its combustor. Therefore, it is important that the propagation of the curved detonation wave should be well understood for the purpose of RDE design.

Many theoretical/experimental studies on steady/quasi-steady curved Zeldovich–von Neumann–Döring (ZND) detonation waves have been performed in the field of condensed-phase explosives [5−12]. However, studies on curved detonation waves of gaseous explosives are scarce, since it is difficult to attain steady curved detonation waves of gaseous explosives. Hence, the propagation characteristics of curved detonation waves of gaseous explosives are not yet sufficiently understood.

Kasahara et al. [13,14] and Maeda et al. [15,16] launched a hypersonic projectile into an explosive gas mixture to generate a steady conical curved detonation wave around the projectile. Although each set of authors mentioned the influence of κ on the stability of the conical curved detonation wave, they could not discuss this issue quantitatively. Kudo et al. [17] demonstrated the steady propagation of a curved detonation wave of C_2H_4+3O_2 stabilized in a rectangular-cross-section curved channel with constant inner/outer radii of curvature, however, they could not obtain the D_n−κ relation of C_2H_4+3O_2. Nakayama et al. [18] used the same gas mixture and simultaneously visualized the front shock and cell structure of a curved detonation wave stabilized in a rectangular-cross-section curved channel with very-shallow depth by employing multi-frame short-time open-shutter photography (MSOP). They showed that the smooth generation of new detonation cells within the enlarged cells stabilizes the propagation of a curved detonation wave and keeps its curved shape smooth [18]. They also formulated a good approximation of the curved shape and showed quantitatively the D_n–κ relation of C_2H_4+3O_2 for the first time [18]. However, their

quantitative examination on the relation was performed at a limited high p_0 (i.e., small λ) since their experimental results were affected by momentum loss due to very-shallow channel depth. Although Nakayama et al. [19] subsequently re-examined the D_n–κ relation by using curved channels with sufficient depth to avoid momentum loss and showed the stabilization condition of curved detonation waves propagating through them, the propagation of curved detonation waves of gaseous explosives was not elucidated sufficiently since only the one gas mixture, $C_2H_4+3O_2$, was used in their study.

Therefore, three types of gas mixture are evaluated under a wide range of initial pressure to investigate extensively the propagation characteristics of a stabilized curved detonation wave in the present study. Rectangular-cross-section curved channels with constant inner/outer radii of curvature are used to stabilize the curved detonation waves like in the previous studies [17−19]. The stabilized curved detonation waves of these gas mixtures are examined to evaluate their D_n−κ relations. The front shock evolution of stabilized curved detonation waves is reconstructed by using these D_n−κ relations and the universal propagation characteristics of the stabilized curved detonation waves are elucidated.

2. Geometric front shock shape of stabilized curved detonation wave in a curved channel

As shown in Fig. 1, the center of the inner/outer radii of curvature of a rectangular-cross-section curved channel is defined as the origin, and the boundary between the curved and straight sections of the curved channel is defined as the initial line in a two-dimensional polar coordinate system. It is assumed that a stabilized curved detonation wave propagates through the curved channel while maintaining a specific curved shape and that ω is time-unvarying as well as constant everywhere on the curved detonation wave. Then, the following differential equation can be established at an arbitrary point P(r,θ) on the curved detonation wave [18,19]:

$$\frac{\mathrm{d}\theta}{\mathrm{d}r} = -\frac{\sqrt{(r\omega)^2 - D_\mathrm{n}^2}}{D_\mathrm{n} r}, \tag{1}$$

where $\omega = D_{\mathrm{n,i}}/r_\mathrm{i}$. If D_n is given as a function of r, the following relation between r and θ, which gives the front shock shape of the curved detonation wave, is derived by integrating Eq. (1) [18,19]:

$$\theta - \theta_\mathrm{i} = -\int_{r_\mathrm{i}}^{r_\mathrm{o}} \frac{\sqrt{(r\omega)^2 - D_\mathrm{n}^2}}{D_\mathrm{n} r}\mathrm{d}r\,. \tag{2}$$

The following formula that approximates a D_n distribution of the curved detonation wave are employed [18,19]:

$$D_\mathrm{n} = D_{\mathrm{n,asy}} - \left(D_{\mathrm{n,asy}} - D_{\mathrm{n,i}}\right)\left(r/r_\mathrm{i}\right)^{-m}, \tag{3}$$

which is applicable only when the reflection over the outer wall is regular. In Eq. (3), D_n increases from $D_{\mathrm{n,i}}$ to $D_{\mathrm{n,asy}}$ asymptotically with increasing r, and the constant m gives the increasing rate of D_n. Generally, the value of $D_{\mathrm{n,asy}}$ is neary equal to that of D_CJ.

As shown in Fig. 1, the front shock shape of the curved detonation wave is divided into fifteen parts at a regular interval in the direction of r. The coordinate values of the division points are picked up, and the front shock shape is defined. The ω values of each division point are determined by observing the moment-to-moment alternation of their positions. The values of $D_{\mathrm{n,asy}}$ and m are determined by the trial-and-error technique in such a way that the residual sum of squares between the reconstructed front shock shape of the curved detonation wave using Eqs. (2) and (3) and the coordinate values of the division points acquired experimentally becomes the smallest [19].

3. Experiment

Figure 2 shows the schematics of the curved channels. Five types of curved channel with different inner radii of curvature are used. The width and depth of these curved channels are 20 mm and 16 mm, respectively. A test gas is filled at a given p_0 in the observation chamber where a curved channel is installed and ignited by a spark plug. A

deflagration wave transitions to a detonation wave within the Shchelkin spiral section located below the curved channel, and a planar detonation wave enters the curved channel.

Table 1 shows the experimental conditions. Three types of stoichiometric test gases, $C_2H_4+3O_2$, $2H_2+O_2$, and $2C_2H_2+5O_2+7Ar$, are used. The λ values are converted from p_0 by using the relations shown in Table 1. These relations are obtained by applying the least-squares method to the data of λ of these test gases extracted from the Detonation Database of Caltech [20]. The velocity of a planar detonation wave entering a curved channel agrees well with D_{CJ} calculated using CEA [21]. Hence, D_{CJ} is used as a reference velocity for the nondimensionalization of D_n.

Detonation waves are visualized by the shadowgraph or schlieren methods and recorded by a high-speed video camera (Shimadzu HPV-2) at 2-μs intervals. The spatial resolution of the photographs taken is approximately 0.3 mm.

4. Results and discussion

4.1. Stabilization condition of curved detonation wave

The propagation mode that consistently satisfies the relation $D_{n,i}/D_{CJ}\geq0.8$ is defined as the stable mode, the mode that cannot satisfy the relation $D_{n,i}/D_{CJ}\geq0.8$ but can consistently satisfy the relation $D_{n,i}/D_{CJ}\geq0.6$ is defined as the critical mode, and the mode in which $D_{n,i}/D_{CJ}<0.6$ even just once is defined as the unstable mode in the present study [18,19]. $D_{n,i}$ is measured at a time interval (Δt) equal to or longer than $2\lambda/D_{CJ}$, and Δt is 2 μs or 4 μs.

Figure 3 shows the relations between r_i and λ in terms of the propagation mode. The propagation mode of a curved detonation wave in a curved channel transitions to the stable mode from the unstable mode approximately within $14\leq r_i/\lambda\leq23$. The lower boundary of stabilization is considered to be about $r_i/\lambda=23$ regardless of the test gas.

The detailed description of the determination method of these boundaries is written in Ref. [18].

Figure 4 is an example of a photograph of a curved detonation wave in the stable mode [19]. This photograph was taken by MSOP [18] using the special curved channel of 1-mm depth. The conditions are $C_2H_4+3O_2$, r_i=20 mm, and λ=0.71 mm. The smooth generation of new detonation cells within the enlarged cells stabilizes the propagation of the curved detonation wave and maintains its smooth curved shape.

4.2. Approximation of front shock shape

The previous studies [18,19] have shown that the propagation of a curved detonation wave in the stable mode eventually becomes steady and that the assumption described in Chapter 2 is correct. This characteristic is absolutely necessary to obtain the $D_n-\kappa$ relation of the curved detonation wave. Figure 5 shows an example of the front shock shape of a curved detonation wave in the stable mode approximated by Eqs. (2) and (3). The conditions are $C_2H_4+3O_2$, r_i=20 mm, and λ=0.70 mm. $D_{n,asy}=0.980D_{CJ}$, m=8.10, $D_{n,i}=0.87235D_{CJ}$, and ω=1.0231x10^5 rad/s are used for the approximation. The error bars represent the typical possible systematic error of measurement resulting from the spatial resolution of the high-speed video camera. The error bars used in figures that follow Fig. 5 represent the same definition. The approximated front shock shape agrees well with the experimental result.

Figure 6 shows an example of the D_n distribution of a curved detonation wave approximated by Eq. (3). The conditions are the same as those in Fig. 5. The approximated distribution of D_n is also in good agreement with the experimental result.

4.3. $D_n/D_{CJ}-\lambda\kappa$ relation

Since the front shock shapes and D_n distribution of curved detonation waves in the stable mode are

approximately given by Eqs. (2) and (3), the $D_n-\kappa$ relations can be obtained from the approximation results of curved detonation waves. Figure 7 shows the $D_n-\kappa$ relations of curved detonation waves in the stable mode. The test gas is $C_2H_4+3O_2$. The values of D_n and κ are nondimensionalized by D_{CJ} and λ, respectively. The ten cases of curved detonation waves at different r_i and/or λ were selected to cover the stable zone shown in Fig. 3a. One can see that D_n/D_{CJ} is a function of $\lambda\kappa$ regardless of the curved channel and that it decreases with increasing $\lambda\kappa$. The same characteristic is also seen in the $D_n/D_{CJ}-\lambda\kappa$ relations of $2H_2+O_2$ and $2C_2H_2+5O_2+7Ar$.

The $D_n/D_{CJ}-\lambda\kappa$ relations of all the test gases are compared in Fig. 8. For each test gas, several cases covering each stable zone in Fig. 3 were selected to evaluate their $D_n/D_{CJ}-\lambda\kappa$ relations. The $D_n/D_{CJ}-\lambda\kappa$ relations of each test gas are approximated by a cubic function. It is noteworthy that the difference in the $D_n/D_{CJ}-\lambda\kappa$ relation of each test gas is very small, and, more specifically, the $D_n/D_{CJ}-\lambda\kappa$ relation does not depend on the type of test gas. Therefore, the average of these $D_n/D_{CJ}-\lambda\kappa$ relations is defined as the overall $D_n/D_{CJ}-\lambda\kappa$ relation and approximated by a cubic function of $D_n/D_{CJ}=\sum a_j(\lambda\kappa)^j$, where j=0−3, a_0=1.0000, a_1=−1.3017, a_2=16.089, and a_3=−169.67.

Figure 9 shows examples of the reconstruction of the front shock behavior of curved detonation waves with the overall $D_n/D_{CJ}-\lambda\kappa$ relation. The marker particle method [22] is employed to track the front shocks of the curved detonation waves. The boundary conditions are set up with the front shock perpendicular to the inner wall and the reflection being regular over the outer wall. The Δt value of the front shocks in the photographs is 2 μs, and that of the reconstructed front shocks is 4 μs. In all the cases, the front shock behavior is successfully reconstructed using the overall $D_n/D_{CJ}-\lambda\kappa$ relation. Hence, once the overall $D_n/D_{CJ}-\lambda\kappa$ relation is given, Eqs. (2) and (3) are no longer necessary. These results show that the propagation behavior of the curved detonation waves is controlled by a specific $D_n/D_{CJ}-\lambda\kappa$relation, therefore detonation shock dynamics (DSD) [5−8] can also be applied to stabilized curved detonation waves of gaseous explosives.

Since the λ–p_0 relations shown in Table 1 are obtained from the data sets with some errors and scatter, the D_n/D_{CJ}–$\lambda\kappa$ relations shown in Fig. 8 may be affected by them. However, it's been confirmed that the front shock behavior of stabilized curved detonation waves can be successfully reconstructed with the overall D_n/D_{CJ}–$\lambda\kappa$ relation also in other conditions as well as in Fig. 9. Hence, one can think that the value of λ given by these relations is appropriate and the influence of these errors and scatter on the results of the present study is small.

4.4. Front shock evolution of curved detonation wave

Figure 10 shows the front shock evolution of curved detonation waves reconstructed with the overall D_n/D_{CJ}–$\lambda\kappa$ relation. Since the condition over the outer wall does not affect the propagation of a curved detonation wave as long as the reflection over the outer wall is regular, r_o is assumed to be infinite in this analysis. Two values of r_i/λ, 23 (lower boundary of stabilization) and 50, are selected. The values of x, y, and t are nondimensionalized as x/r_i, y/r_i, and $tD_{CJ}/r_i(\equiv\tau)$, respectively. The $\Delta\tau$ between front shocks is 1. If the propagation of curved detonation waves in the stable mode is controlled by a specific D_n/D_{CJ}–$\lambda\kappa$ relation, the front shock shapes of the curved detonation waves with the same r_i/λ become congruent on the x/r_i–y/r_i plane at a given τ, regardless of r_i (i.e., the channel type). That is to say, self-similarity is seen in the front shock shapes with the same r_i/λ. The front shock shapes are obviously determined independently from the type of gas mixture if the specific D_n/D_{CJ}–$\lambda\kappa$ relation is unique. The constant $\lambda\kappa$ and D_n/D_{CJ} lines become concentric as the curved detonation waves propagate. This means the curved detonation waves eventually attain a specific curved shape and their propagation becomes steady. The curved shapes develop fully within shorter τ in the curved channel with smaller r/r_i (i.e., a shallower channel). One can predict that the propagation of the curved detonation wave with infinite r_i/λ approaches the Huygens construction asymptotically since the D_n/D_{CJ} deficit and $\lambda\kappa$ decrease with increasing r_i/λ.

Figure 11 shows the comparison of the front shock shapes of curved detonation waves with different r_i. The conditions are $C_2H_4+3O_2$ and r_i/λ=36.3. The experimental result also shows that the front shock shapes with the same r_i/λ become similar regardless of r_i (i.e., the channel type). The values of $D_{n,asy}$ and m determined from the approximation by Eqs. (2) and (3) are $0.965D_{CJ}$ and 10.25 for r_i=20 mm, $0.970D_{CJ}$ and 11.00 for r_i=40 mm, and $0.970D_{CJ}$ and 10.55 for r_i=60 mm, respectively. The differences in $D_{n,asy}/D_{CJ}$ and m between the different r_i are very small, and hence this result also supports the self-similarity shown in Fig. 11.

Figure 12 shows the comparison of the front shock shapes of curved detonation waves with different test gases. The conditions are r_i=20 mm and r_i/λ=27.5. The experimental result also shows that the front shock shapes with the same r_i/λ are determined independently from the type of test gas and they are similar. The values of $D_{n,asy}$ and m determined from the approximation by Eqs. (2) and (3) are $0.985D_{CJ}$ and 7.70 for $C_2H_4+3O_2$, $0.970D_{CJ}$ and 0.75 for $2H_2+O_2$, and $0.980D_{CJ}$ and 7.50 for $2C_2H_2+5O_2+7Ar$, respectively. The differences in $D_{n,asy}/D_{CJ}$ and m between the different test gases are very small, and hence this result also supports the self-similarity between them.

5. Conclusions

The propagation of curved detonation waves of gaseous explosives stabilized in rectangular-cross-section curved channels was investigated. The lower boundary of stabilization is around r_i/λ=23 regardless of the test gas used in the present study. The D_n/D_{CJ} of a stabilized curved detonation wave is a function of the $\lambda\kappa$, and the D_n/D_{CJ}–$\lambda\kappa$ relation does not depend on the type of test gas. The front shock evolution of the stabilized curved detonation waves is controlled by the D_n/D_{CJ}–$\lambda\kappa$ relation. Due to this propagation characteristic, the stabilized curved detonation waves eventually propagate steadily through the curved channels while maintaining a specific curved shape. Self-similarity is seen in the front shock shapes of the stabilized curved detonation waves with the same r_i/λ

regardless of the curved channel and test gas.

Acknowledgements

This work was supported by Grants-in-Aid for Scientific Research (A) (No.20241040) and (B) (No.21360411), MEXT, and by the Research Grant Program, ISAS/JAXA.

References

[1] M. Hishida, T. Fujiwara, P. Wolański, Shock Waves 19 (2009) 1-10.

[2] J. Kindracki, P. Wolański, Z. Gut, Shock Waves 21 (2011) 75-84.

[3] Y. Eude, D.M. Davidenko, I. Gökalp, F. Falempin, AIAA Paper 2011-2236, 2011.

[4] T. Yamada, A.K. Hayashi, E. Yamada, N. Tsuboi, V.E. Tangirala, T. Fujiwara, Combust. Sci. and Tech. 182 (2010) 1901-1914.

[5] J.B. Bdzil, D.S. Stewart, Phys. Fluids A 1 (7) (1989) 1261-1267.

[6] D.S. Stewart, J.B. Bdzil, Combust. Flame 72 (1988) 311-323.

[7] D.S. Stewart, J. Yao, W.C. Davis, Proc. Combust. Inst. 28 (2000) 619-628.

[8] D.E. Lambert, D.S. Stewart, S. Yoo, B.L. Wescott, J. Fluid Mech. 546 (2006) 227-253.

[9] M. Short, G.J. Sharpe, V. Gorchkov, J.B Bdzil, Proc. Combust. Inst. 30 (2005) 1899-1906.

[10] J. Yao, D.S. Stewart, Combust. Flame 100 (1995) 519-528.

[11] B.L. Wescott, D.S. Stewart, W.C. Davis, J. Appl. Phys. 98, 053514 (2005).

[12] S.I. Jackson, C.B. Kiyanda, M. Short, Proc. Combust. Inst. 33 (2011) 2219-2226.

[13] J. Kasahara, T. Fujiwara, T. Endo, T. Arai, AIAA Journal 39 (8) (2001) 1553-1561.

[14] J. Kasahara, T. Arai, S. Chiba, K. Takazawa, Y. Tanahashi, A. Matsuo, Proc. Combust. Inst. 29 (2002) 2817-2824.

[15] S. Maeda, R. Inada, J. Kasahara, A. Matsuo, Proc. Combust. Inst. 33 (2011) 2343-2349.

[16] S. Maeda, J. Kasahara, A. Matsuo, Combust. Flame 159 (2012) 887-896.

[17] Y. Kudo, Y. Nagura, J. Kasahara, Y. Sasamoto, A. Matsuo, Proc. Combust. Inst. 33 (2011) 2319-2326.

[18] H. Nakayama, T. Moriya, J. Kasahara, A. Matsuo, Y. Sasamoto, I. Funaki, Combust. Flame 159 (2012) 859-869.

[19] H. Nakayama, T. Moriya, J. Kasahara, A. Matsuo, Y. Sasamoto, I. Funaki, Propagation of Curved Detonation Waves Stabilized in Annular Channels with a Rectangular Cross-section, Trans. JSASS Aerospace Tech. Japan (in press).

[20] M. Kaneshige, J.E. Shepherd, Detonation Database, Technical Report FM97-8, GALCIT, 1997, available at http://www.galcitt.caltech.edu/detn_db/html/db.html.

[21] S. Gordon, B.J. McBride, Computer Program for Calculation of Complex Chemical Equilibrium Compositions and Applications, RP-1311, NASA, 1994.

[22] J.A. Sethian, Level Set Methods and Fast Marching Methods, Cambridge University Press, Cambridge, U.K., 1999, pp. 34-38.

Table title and figure captions

Table 1 Experimental conditions (temperature is 298±6 K).

Fig. 1. Geometric relationship in a curved detonation wave stabilized in a rectangular-cross-section curved channel.

Fig. 2. Schematics of curved channels.

Fig. 3. Relations between r_i and λ in terms of the propagation mode.

Fig. 4. MSOP photograph of a curved detonation wave in the stable mode [19].

Fig. 5. Approximated front shock shape of a curved detonation wave in the stable mode (C_2H_4+3O_2, r_i=20 mm, λ=0.70 mm, $D_{n,asy}$=0.980D_{CJ}, m=8.10, $D_{n,i}$=0.87235D_{CJ}, ω=1.0231x10^5 rad/s).

Fig. 6. Approximated D_n distribution of a curved detonation wave in the stable mode (C_2H_4+3O_2, r_i=20 mm, λ=0.70 mm, $D_{n,asy}$=0.980D_{CJ}, m=8.10, $D_{n,i}$=0.87235D_{CJ}, ω=1.0231x10^5 rad/s).

Fig. 7. D_n/D_{CJ}–$\lambda\kappa$ relations of curved detonation waves in the stable mode (C_2H_4+3O_2).

Fig. 8. Comparison of the D_n/D_{CJ}–$\lambda\kappa$ relations.

Fig. 9. Reconstruction of the front shock behavior of curved detonation waves with the overall D_n/D_{CJ}–$\lambda\kappa$ relation.

Fig. 10. Front shock evolution of curved detonation waves reconstructed with the overall D_n/D_{CJ}–$\lambda\kappa$ relation (r_i/λ=23 and r_i/λ=50).

Fig. 11. Self-similarity of the front shock shapes of curved detonation waves with different r_i (C_2H_4+3O_2, r_i/λ=36.3).

Fig. 12. Self-similarity of the front shock shapes of curved detonation waves with different test gases (r_i=20 mm, r_i/λ=27.5).

Table 1

Experimental conditions (temperature is 298±6 K).

Test gas	p_0 (kPa)	λ (mm)[a]	D_{CJ} (m/s)[b]
$C_2H_4+3O_2$	20−100	0.40−2.41	2296−2376
$2H_2+O_2$	30−190	0.73−4.82	2772−2873
$2C_2H_2+5O_2+7Ar$	15−150	0.23−3.00	1928−2033

[a] Detonation Database, Caltech [20]

$C_2H_4+3O_2$: $\lambda = 72.020 p_0^{-1.1270}$ (SD: 18%)

$2H_2+O_2$: $\lambda = 157.15 p_0^{-1.0242}$ (SD: 22%)

$2C_2H_2+5O_2+7Ar$: $\lambda = 61.522 p_0^{-1.1173}$ (SD: 7%)

[b] CEA, NASA [21]

(11 text lines + 2 blanks) x 7.6 words/line x 1 column = 99 words

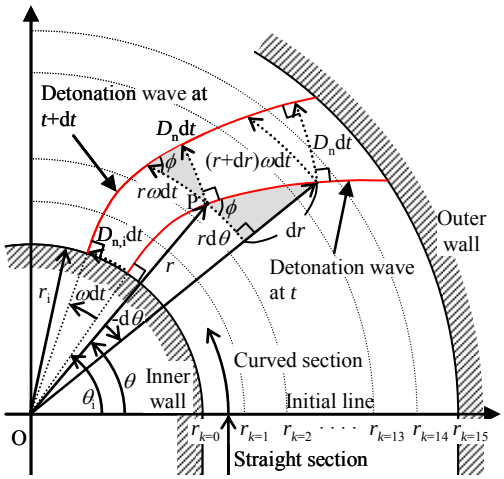

Fig. 1. Geometric relationship in a curved detonation wave stabilized in a rectangular-cross-section curved channel.

M1: (62 mm + 10 mm) x 2.2 words/mm x 1 column + 13 words = 171 words

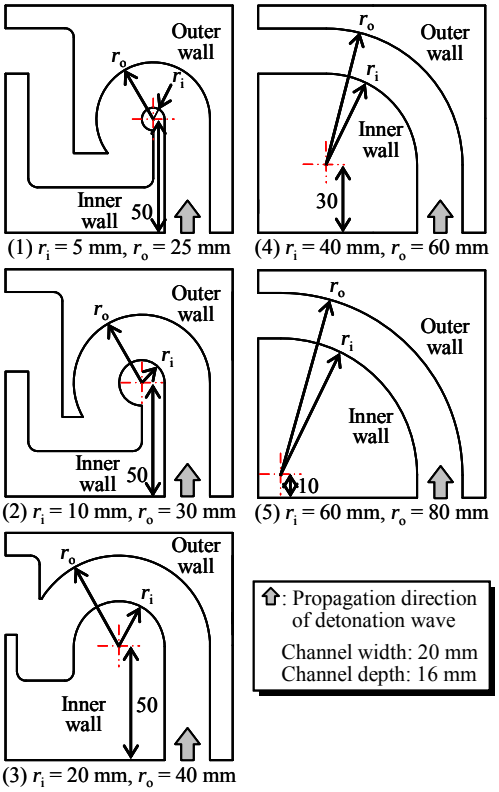

Fig. 2. Schematics of curved channels.

M1: (104 mm + 10 mm) x 2.2 words/mm x 1 column + 4 words = 255 words

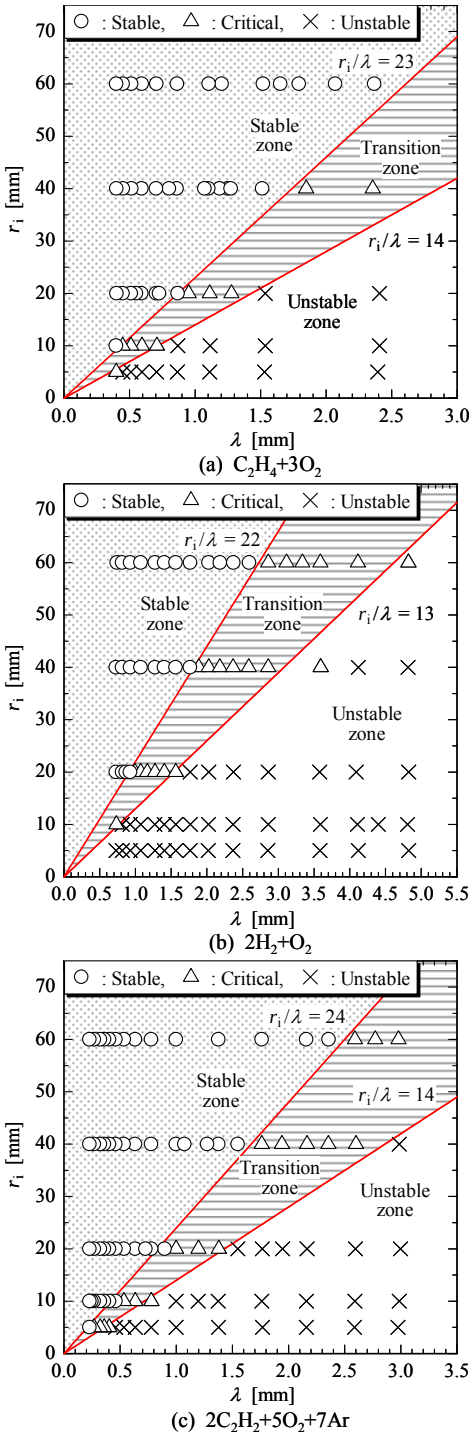

Fig. 3. Relations between r_i and λ in terms of the propagation mode.

M1: (189 mm + 10 mm) x 2.2 words/mm x 1 column + 11 words = 449 words

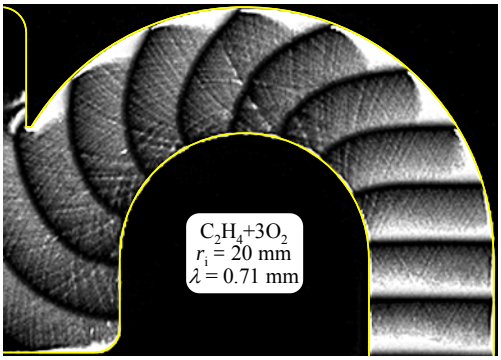

Fig. 4. MSOP photograph of a curved detonation wave in the stable mode [19].

M1: (47 mm + 10 mm) x 2.2 words/mm x 1 column + 12 words = 137 words

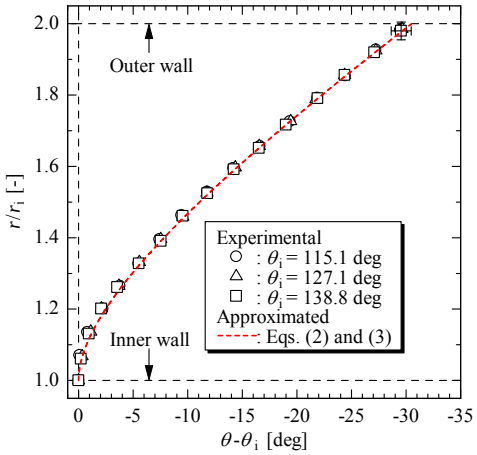

Fig. 5. Approximated front shock shape of a curved detonation wave in the stable mode (C_2H_4+3O_2, r_i=20 mm, λ=0.70 mm, $D_{n,asy}$=0.980D_{CJ}, m=8.10, $D_{n,i}$=0.87235D_{CJ}, ω=1.0231x10^5 rad/s).

M1: (59 mm + 10 mm) x 2.2 words/mm x 1 column + 23 words = 175 words

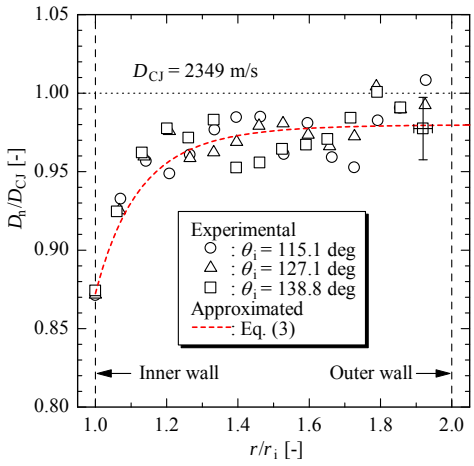

Fig. 6. Approximated D_n distribution of a curved detonation wave in the stable mode (C_2H_4+3O_2, r_i=20 mm, λ=0.70 mm, $D_{n,asy}$=0.980D_{CJ}, m=8.10, $D_{n,i}$=0.87235D_{CJ}, ω=1.0231x10^5 rad/s).

M1: (60 mm + 10 mm) x 2.2 words/mm x 1 column + 22 words = 176 words

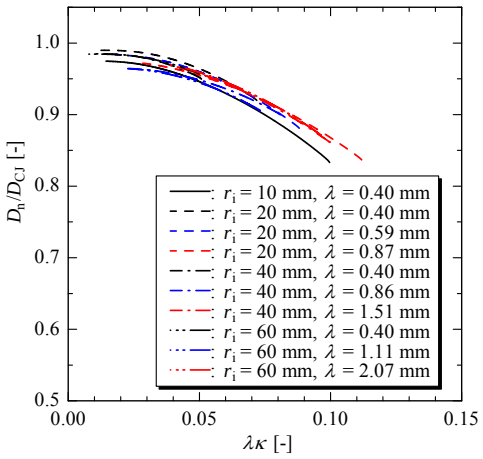

Fig. 7. D_n/D_{CJ}–$\lambda\kappa$ relations of curved detonation waves in the stable mode (C_2H_4+3O_2).

M1: (59 mm + 10 mm) x 2.2 words/mm x 1 column + 11 words = 163 words

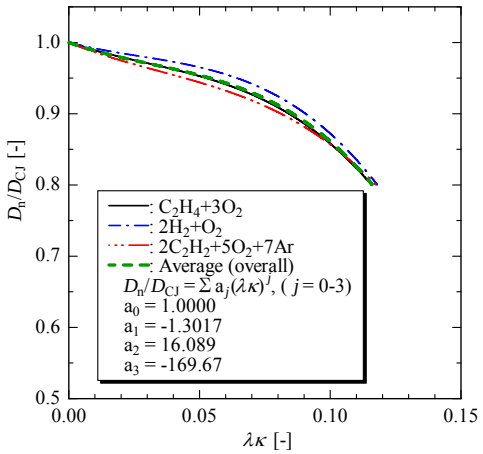

Fig. 8. Comparison of the D_n/D_{CJ}–$\lambda\kappa$ relations.

M1: (59 mm + 10 mm) x 2.2 words/mm x 1 column + 5 words = 157 words

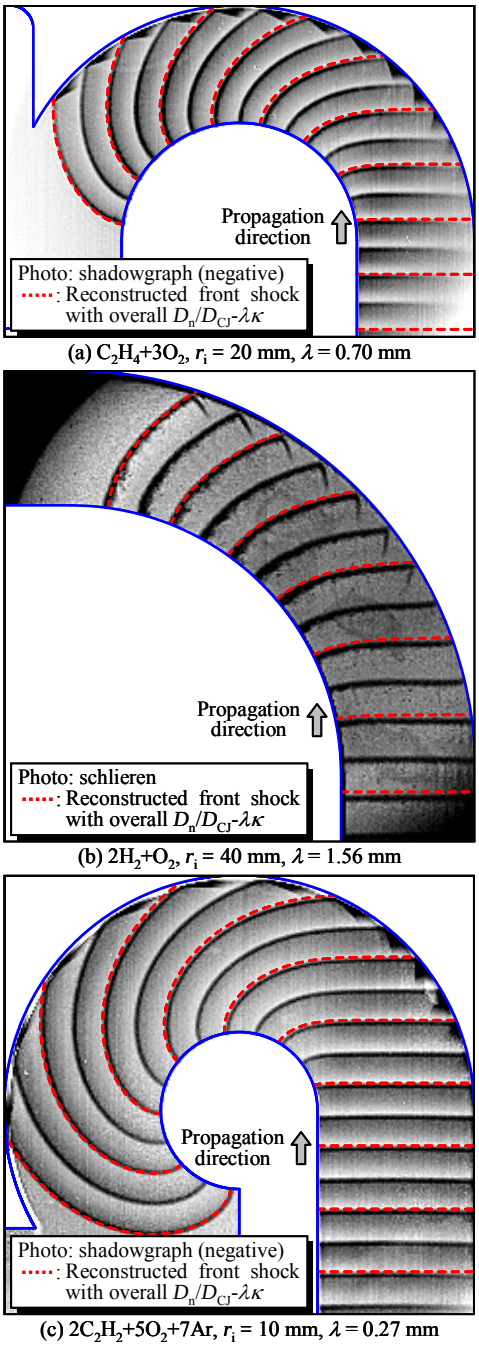

Fig. 9. Reconstruction of the front shock behavior of curved detonation waves with the overall D_n/D_{CJ}–$\lambda\kappa$ relation.

M1: (177 mm + 10 mm) x 2.2 words/mm x 1 column + 15 words = 426 words

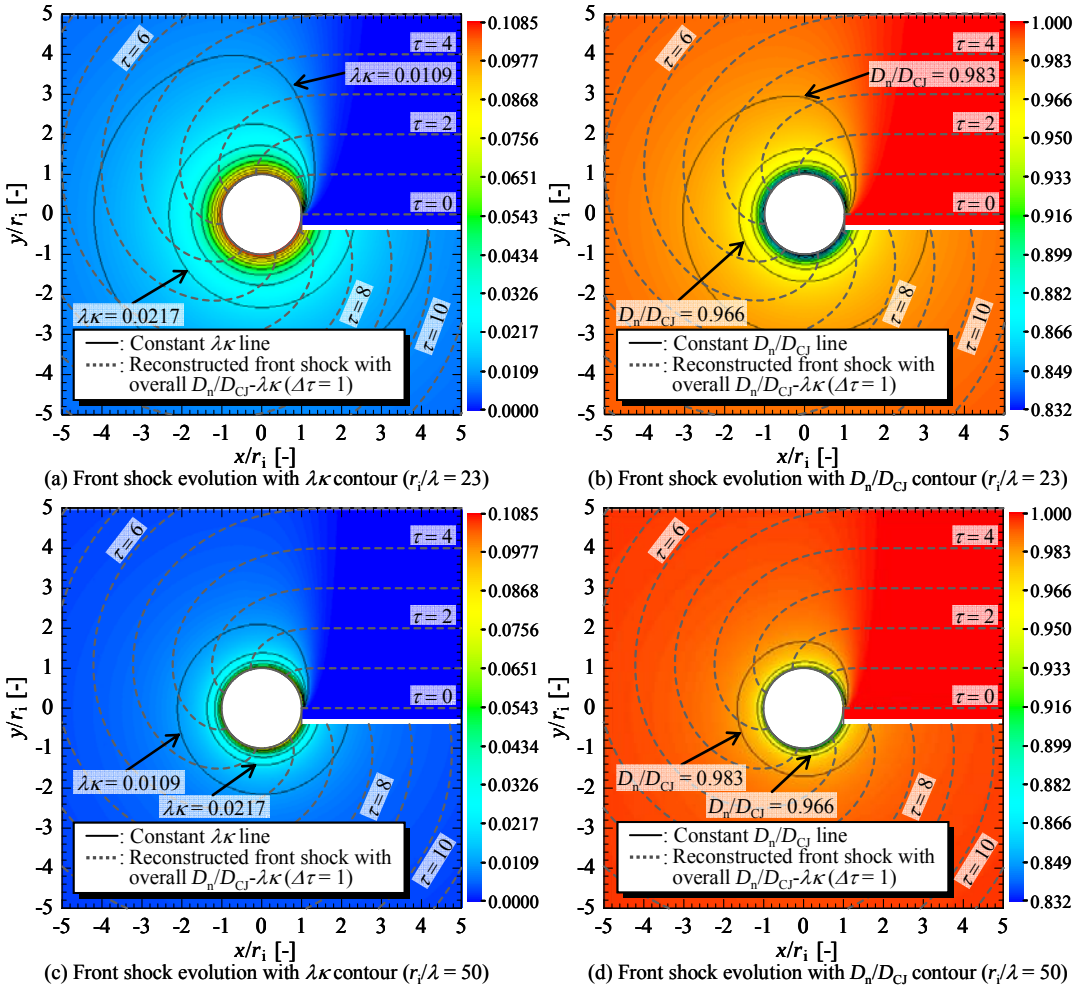

(a) Front shock evolution with $\lambda\kappa$ contour ($r_i/\lambda = 23$)

(b) Front shock evolution with D_n/D_{CJ} contour ($r_i/\lambda = 23$)

(c) Front shock evolution with $\lambda\kappa$ contour ($r_i/\lambda = 50$)

(d) Front shock evolution with D_n/D_{CJ} contour ($r_i/\lambda = 50$)

Fig. 10. Front shock evolution of curved detonation waves reconstructed with the overall D_n/D_{CJ}–$\lambda\kappa$ relation (r_i/λ=23 and r_i/λ=50).

M1: (130 mm + 10 mm) x 2.2 words/mm x 2 column + 16 words = 632 words

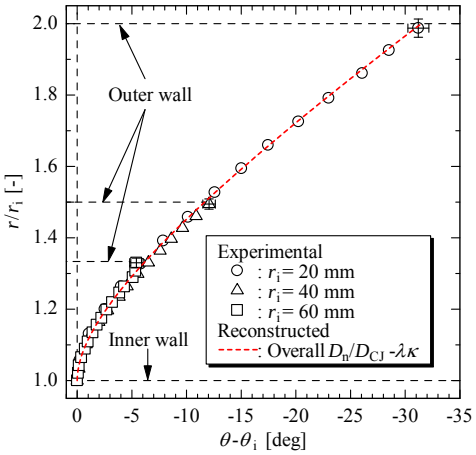

Fig. 11. Self-similarity of the front shock shapes of curved detonation waves with different r_i (C_2H_4+3O_2, r_i/λ=36.3).

M1: (59 mm + 10 mm) x 2.2 words/mm x 1 column + 15 words = 167 words

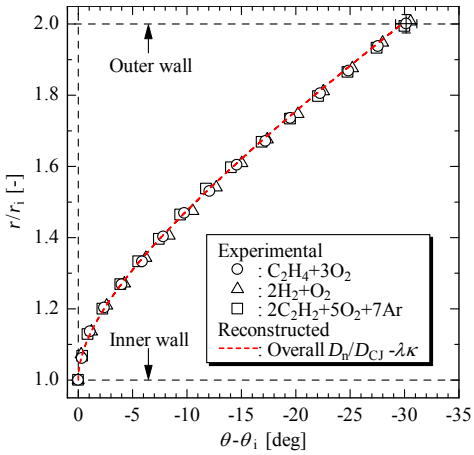

Fig. 12. Self-similarity of the front shock shapes of curved detonation waves with different test gases (r_i=20 mm, r_i/λ=27.5).

M1: (59 mm + 10 mm) x 2.2 words/mm x 1 column + 17 words = 169 words